

Variability of Microphysical Parameters in High-Altitude Ice Clouds: Results of the Remote Sensing Method

SERGEY Y. MATROSOV

*Cooperative Institute for Research in Environmental Sciences, University of Colorado and NOAA
Environmental Technology Laboratory, Boulder, Colorado*

(Manuscript received 22 April 1996, in final form 23 October 1996)

ABSTRACT

The remote sensing method for retrieving vertical profiles of microphysical parameters in ice clouds from ground-based measurements taken by the Doppler radar and IR radiometer was applied to several cloud cases observed during different field experiments including FIRE-II, ASTEX, and the Arizona Program. The measurements were performed with the NOAA Environmental Technology Laboratory instrumentation. The observed ice clouds were mostly cirrus clouds located in the upper troposphere above 5.6 km. Their geometrical thicknesses varied from a few hundred meters to 3 km. Characteristic cloud particle sizes expressed in median mass diameters of equal-volume spheres varied from about 25 μm to more than 400 μm . Typically, characteristic particle sizes were increasing toward the cloud base, with the exception of the lowest range gates where particles were quickly sublimating. Highest particle concentrations were usually observed near the cloud tops. The vertical variability of particle sizes inside an individual cloud could reach one order of magnitude. The standard deviation of the mean profile for a typical cloud is usually factor of 2 or 3 smaller than mean values of particle characteristic size. Typical values of retrieved cloud ice water content varied from 1 to 100 mg m^{-3} ; however, individual variations were as high as four orders of magnitude. There was no consistent pattern in the vertical distribution of ice water content except for the rapid decrease in the vicinity of the cloud base. The relationships between retrieved cloud parameters and measured radar reflectivities were considered. The uncertainty of estimating cloud parameters from the power-law regressions is discussed. The parameters of these regressions varied from cloud to cloud and were comparable to the parameters in corresponding regressions obtained from direct particle sampling in other experiments. Relationships between cloud microphysical parameters and reflectivity can vary even for the same observational case. The variability diminishes if stronger reflectivities are considered. A procedure of "tuning" cloud microphysics–reflectivity regressions for individual profiles is suggested. Such a procedure can simplify the radar–radiometer method and make it applicable for a broader range of clouds.

1. Introduction

The importance of clouds in the radiation budget of the earth is widely recognized. Clouds influence and interact with both incoming solar radiation and outgoing thermal terrestrial radiation. Cloud radiative properties are determined by their microphysics (e.g., particle size distribution, their shape and phase) and macrophysics (e.g., thickness, horizontal extent, cloud height). Our current knowledge of cloud properties and their variabilities is still insufficient to model the cloud radiative impact on the earth climate system in a correct, quantitative way. A combination of new, detailed studies of clouds from different observational platforms (e.g., satellite, aircraft, balloon, ground) is necessary to improve our current understanding of cloud formation mechanisms, their microphysics, and their radiative feedbacks in the climate system (Hobbs 1993).

Remote sensing methods have been used extensively in cloud microphysical research during the last few decades, and new techniques are being developed. One of the important advantages of remote sensing approaches over direct aircraft or balloon-based cloud sampling techniques is a much greater coverage both in space and time. This eventually can lead to acquiring representative statistics about cloud properties, which are important for better understanding the role of clouds in the earth climate. However, the accuracy of the remote sensing measurements and its dependence on a priori assumptions should be understood.

New remote sensing developments utilize more advanced instruments and are often based on the use of several different remote sensors and/or a multiwavelength approach. Multisensor and/or multiwavelength approaches usually help to avoid some potential retrieval ambiguities that would otherwise exist if only a single remote sensor operating at one wavelength were used. These ambiguities are almost inevitable for the single-remote-sensor approach because generally there is no direct correspondence between any cloud microphysical

Corresponding author address: Dr. Sergey Y. Matrosov, NOAA/ERL/ETL, Mailcode R/E/ET6, 325 Broadway, Boulder, CO 80303.
E-mail: smatrosov@etl.noaa.gov

parameters of interest and a single measurable taken by any remote sensor at one wavelength.

Active remote sensors such as lidar and radar provide vertically resolved information about cloud structure. Low atmospheric attenuation of radar signals makes radar a promising means for cloud studies. This results in recent developments of several millimeter-wavelength radar systems dedicated primarily to the cloud research (Kropfli et al. 1995; Mead et al. 1994; Clothiaux et al. 1995). Compared to conventional centimeter-wavelength weather radars, millimeter-wavelength radars are inherently more sensitive to small cloud particles, provide a better spatial resolution, and have a better signal-to-clutter ratio (Kropfli and Kelly 1996). These features make these radars very useful tools for studies of nonprecipitating clouds.

This paper summarizes some recent results of the microphysical retrievals of ice cloud parameters using ground-based remote sensors from the Radar Division of the NOAA Environmental Technology Laboratory (ETL). The instrumentation used for these studies included the K_a -band ($\lambda \approx 8.6$ mm) Doppler radar with changeable polarization; a narrowband Barnes model PRT-5 radiometer ($\lambda \sim 10$ – 11.4 μm); and a two-channel (20.6 and 31.6 GHz) microwave (MW) radiometer. The description of the instruments is given in more detail by Intrieri et al. (1995).

ETL participated with this instrumentation in several recent cloud field projects. These projects were conducted in various geographical locations and during different seasons. They included the First International Satellite Cloud Climatology Project (ISCCP) Regional Experiment-Phase II (FIRE-II) at Coffeyville, Kansas, in November 1991 (Stephens 1995), the Atlantic Stratocumulus Transition Experiment (ASTEX) in Porto Santo, Madeira, Portugal, in June 1992 (Randall 1995), and the 1995 Arizona Program in Cottonwood, Arizona, during January–March 1995 (Klimowski 1995). While ice clouds were the primary goal of studies in FIRE-II, ASTEX and Arizona Program projects were devoted mainly to the marine stratocumulus clouds and Mogollon Plateau winter storms, respectively. However, a number of nonprecipitating high-altitude ice cloud cases were observed during the later two projects as well.

Several ice cloud cases observed in the projects mentioned above were analyzed. The remote sensing method was applied to these datasets. As a result, time series of vertical profiles of cloud microphysical parameters such as cloud ice mass content, characteristic particle size, and number concentration were retrieved from ground-based measurements for these cases.

The observed clouds comprised mostly cirrus clouds as well as some clouds observed at altitudes somewhat lower than the ones usually associated with classic cirrus clouds. However, all the observed clouds consisted of predominantly ice phase (as indicated by the MW radiometer). Their altitudes varied from about 5.6 to 11 km above the ground and temperatures were generally

colder than -20°C . Only clouds without strong turbulence (large values of the second Doppler moment) were considered for these retrievals. Typical values of vertical Doppler velocities measured in clouds were within 1 m s^{-1} .

2. Brief description of the retrieval method

The remote sensing method used here to retrieve microphysical properties of ice clouds is based on combined radar and radiometer measurements taken by vertically pointed instruments. This method is best suited for clouds when their dynamic structure is not very intense. The general description of the method was given by Matrosov et al. (1994) and Matrosov et al. (1995). Some modifications in the retrieval algorithm were introduced since then, so the outline of this algorithm is briefly described here.

Radar measurables used in the retrievals are radar reflectivity Z_e and Doppler velocity V_D , measured in each range gate with typical spacing of $\Delta h = 37.5$ m. Time averaging (1–3 h) is used to ensure that residual vertical air motions are small (a few centimeters per second) compared to ice cloud particle fall velocities V_i , which have typical values ranging from about 10 cm s^{-1} to almost 1 m s^{-1} . A multiple regression between V_i , Z_e , and height within a cloud h is then constructed for each observational case to get estimates of vertical profiles of instantaneous reflectivity-weighted particle fall velocities V_i (Orr and Kropfli 1993). Observational cases with large standard deviations of such a regression, as well as cases with large residual vertical air motions, were not used for microphysical retrievals. Retrieval uncertainties caused by residual vertical air motions of an order of a few centimeters per second are usually small. They are discussed by Matrosov et al. (1995) in application for one of the observational cases from FIRE-II. Vertical air motions inside the cloud during this case were simultaneously and independently measured by a 404-MHz wind profiler.

Infrared radiometer brightness temperatures T_b are used to estimate cloud infrared absorption optical thickness τ_a from

$$B(T_b) = B(T_e)[1 - \exp(-\tau_a) + \delta\epsilon]P_a + (1 - P_a)B(T_a) + R_g, \quad (1)$$

where B is the Planck function for the middle of the PRT-5 wavelength band. Being an important radiative cloud parameter, τ_a is also used to normalize vertical profiles of cloud absorption coefficients, which are one of the outputs of the discussed retrieval method. The scheme to infer optical thickness values from measurements of IR brightness temperatures accounts for multiple scattering ($\delta\epsilon$), the reflection of the ground radiation (R_g), changes of the effective radiating cloud temperature (T_e) depending on τ_a and the transmittance (P_a), and the emittance of the intervening atmosphere. The

transmittance P_a depends mostly on the integrated amount of water vapor. It was adjusted continuously based on measurements taken by an ETL three-channel microwave radiometer. In more detail, the optical thickness estimation scheme is described by Matrosov et al. (1995). The derivations of $\delta\epsilon$ and T_e are given by Matrosov and Snider (1995), and the derivation of R_g is given by Platt and Dilley (1979).

Microwave radiometer measurements are used primarily to get an indication of presence of liquid water in predominantly ice phase clouds and to obtain the amount of atmospheric water vapor needed for accounting for the atmospheric effects when inferring cloud optical thickness. Estimations of τ_a using this scheme are possible when $\tau_a \leq 3$. For greater optical thicknesses, brightness temperatures approach to the cloud thermodynamic temperatures. This prevents inferring τ_a from thermal emission measurements.

Combining radar and radiometer measurements, one gets $2L + 1$ observables for each radar beam, where L is the number of range gates. Those observables are L values of measured reflectivity Z_e , L values of estimated reflectivity-weighted particle terminal velocities V_r , and one estimated value of cloud optical thickness. For the assumed type of particle size distribution (typically gamma functions), these observables can be related to unknown particle number concentration N and characteristic size D_m at each range gate by means of a nonlinear system of algebraic equations:

$$\tau_a = \sum_i k_1(\rho, r, n, D_{mi}) N_i D_{mi}^2 \Delta h_i, \quad (2)$$

$$Z_{ei} = k_2(\rho, r, n, D_{mi}) N_i D_{mi}^6, \quad (3)$$

$$V_{ri} = A k_3(\rho, r, n, D_{mi}) D_{mi}^B, \quad (4)$$

where coefficients k_1 , k_2 , and k_3 depend on a priori assumptions about particle density ρ , the order of the gamma size distribution n , and particle aspect ratio r . The summation in (2) is over all L range gates within a cloud, and (3) and (4) are written for an individual range gate, i . Note that this system can also be written in terms of D_m and ice water content (IWC).

The coefficients A and B in (4) depend on particle habits and sizes (Mitchell 1996). While the exponent B exhibits a quite modest dependence on these parameters being around 1 and diminishing with the particle size increase, the coefficient A changes more significantly and is regarded as unknown in the retrieval algorithm. In the current version of the method, B is assumed to depend on D_m and vary from 1.1 for smallest detectable characteristic sizes ($\sim 20 \mu\text{m}$) to 0.9 for the largest D_m .

Equations (2) through (4) are written in terms of a characteristic particle size that can be chosen differently. The size D_m in these equations now is the median mass diameter of the equal-volume sphere. This characteristic size has a simple meaning: IWC (sometimes this parameter is called ice mass content—IMC) in particles that are less than D_m is equal to IWC in those that sizes

are greater than D_m . For the first-order gamma distribution of particles of the same density, D_m is about 2.4 times greater than another widely used characteristic particle size, effective radius r_e ($D_m \approx 2.4r_e$). For the exponential distribution the corresponding coefficient is about 2.5.

The discussed remote sensing approach considers nonspherical cloud particles of planar and/or columnar types with minor to major dimension ratio r . Direct microphysical sampling suggests that particles less than about $100 \mu\text{m}$ could be assumed to have density of solid ice (0.9 g cm^{-3}). The effective density of larger particles diminishes as their size increases. It is currently assumed that for those particles the effective density (g cm^{-3}) can be approximated by the equation:

$$\rho = 0.07D^{-1.1}, \quad (5)$$

where D (mm) is the size of an individual particle. Brown and Francis (1995) found this approximation to be generally suitable for cirrus cloud particles.

The coefficients k_1 and k_2 in (2) and (3) are calculated for an assumed size distribution type using anomalous diffraction theory for the absorption coefficient [Eq. (2)] (Chylek and Videen 1994) and the Rayleigh scattering theory [Eq. (3)] for nonspherical particles. Particles are assumed to be spheroidal and randomly oriented with their major dimensions in the horizontal plane. The coefficient k_3 represents reflectivity weighting of the size-fall velocity relationship for cloud particles. The size distribution of cloud particles in terms of diameters of equal-volume spheres (D) is approximated by the gamma distribution $\{N_0 D^n \exp[-(3.67 + n)D/D_o]\}$, where D_o is the median volume diameter. For the retrievals shown here the order of the distribution n was assumed to be 1. The first-order gamma distribution usually satisfactorily describes the experimental spectra of high-altitude ice cloud particles (Kosarev and Mazin 1989).

The system (2)–(4) is solved iteratively for each vertical radar beam. The output information includes vertical profiles of D_m , IWC, and N . Five to seven iterations are usually enough to ensure the convergence of the solution.

3. Example of time–height cross sections of cloud properties

Figure 1 shows examples of applying the radar–radiometer method in one experimental situation. This example represents an ice cloud observed on 23 June 1992 during ASTEX. The cloud was quite mature, and its thickness varied from 1 to about 3 km during the 2-h observation period. Radar reflectivity values measured in this cloud are shown in Fig. 1a. During times shown blank, the radar was in a scanning mode and its data were not used in retrievals.

Vertically averaged reflectivities for this case varied from -5 to -11 dBZ, which is about 10 – 15 dBZ higher than for a typical cirrus cloud. The strongest reflectivity

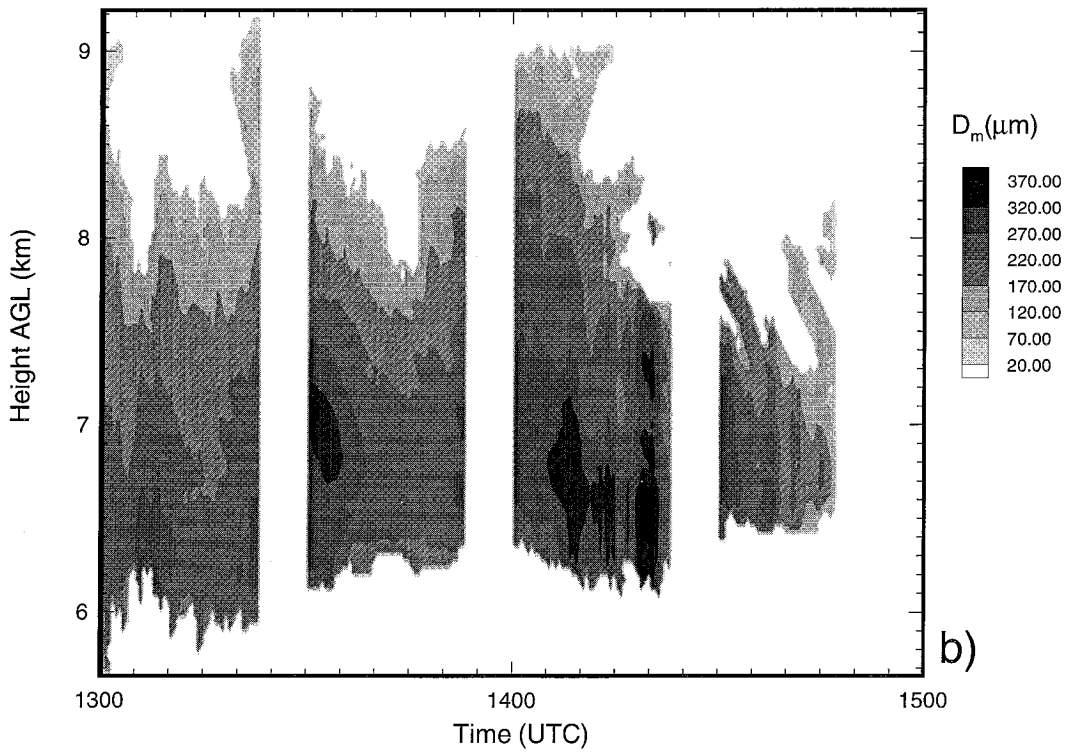
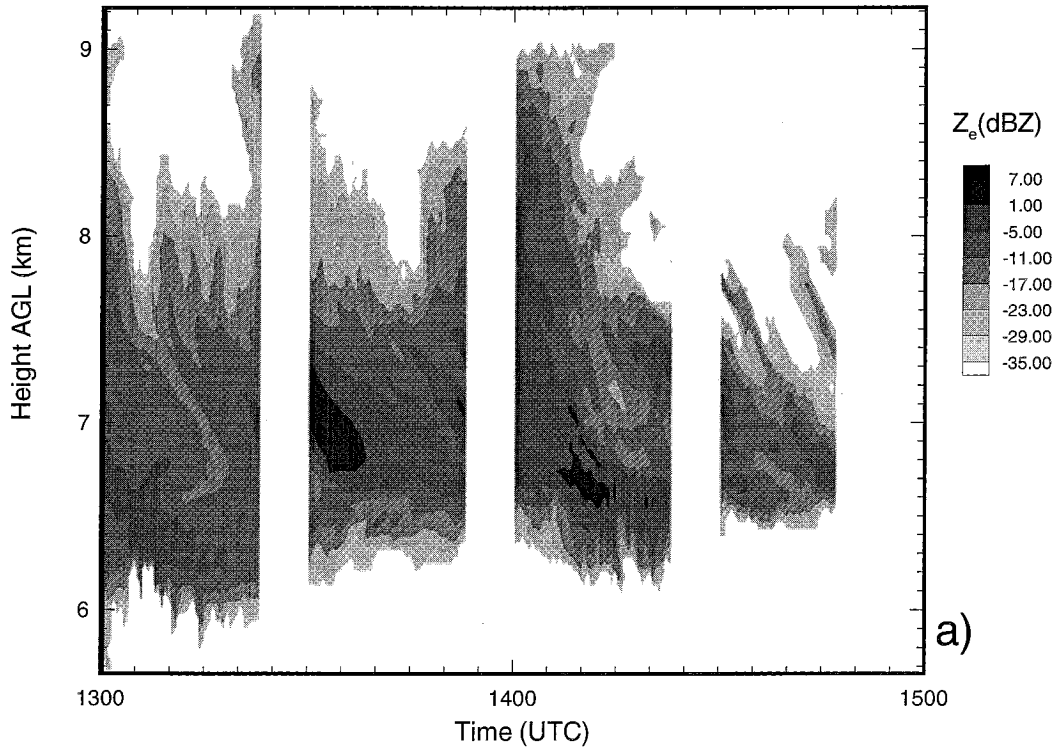


FIG. 1. The time–height cross sections of measured radar reflectivity (a), retrieved median mass sizes of cloud particles D_m (b), and cloud ice water content (c), their concentrations N (d), in the cloud observed on 23 June 1992 during ASTEX.

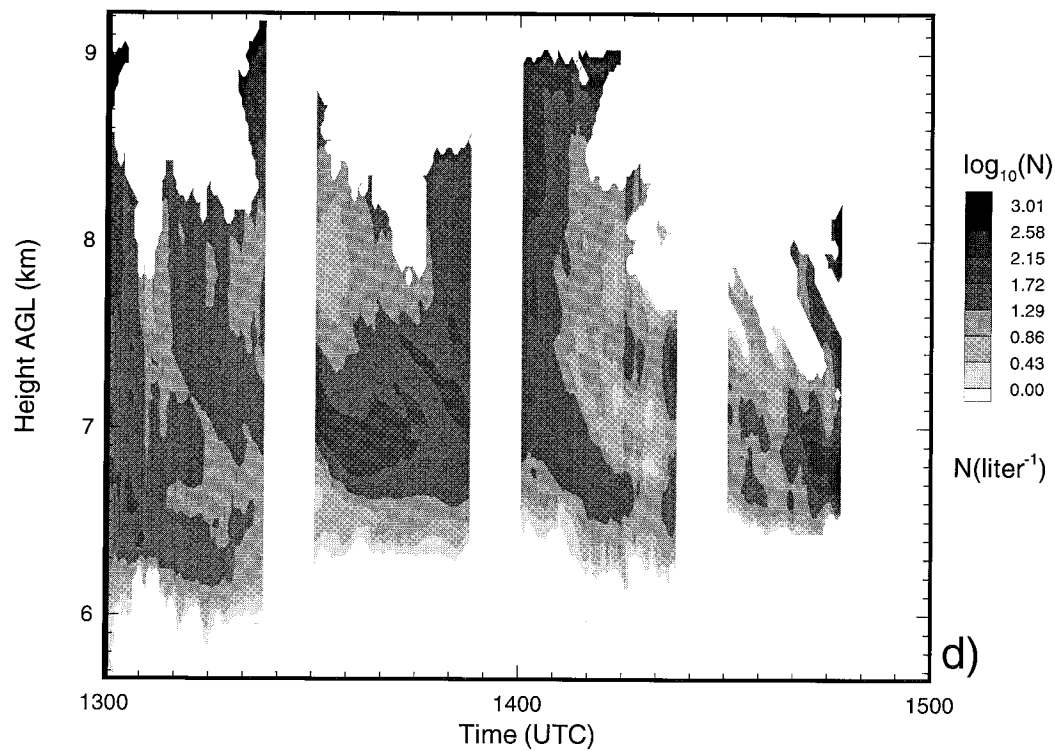
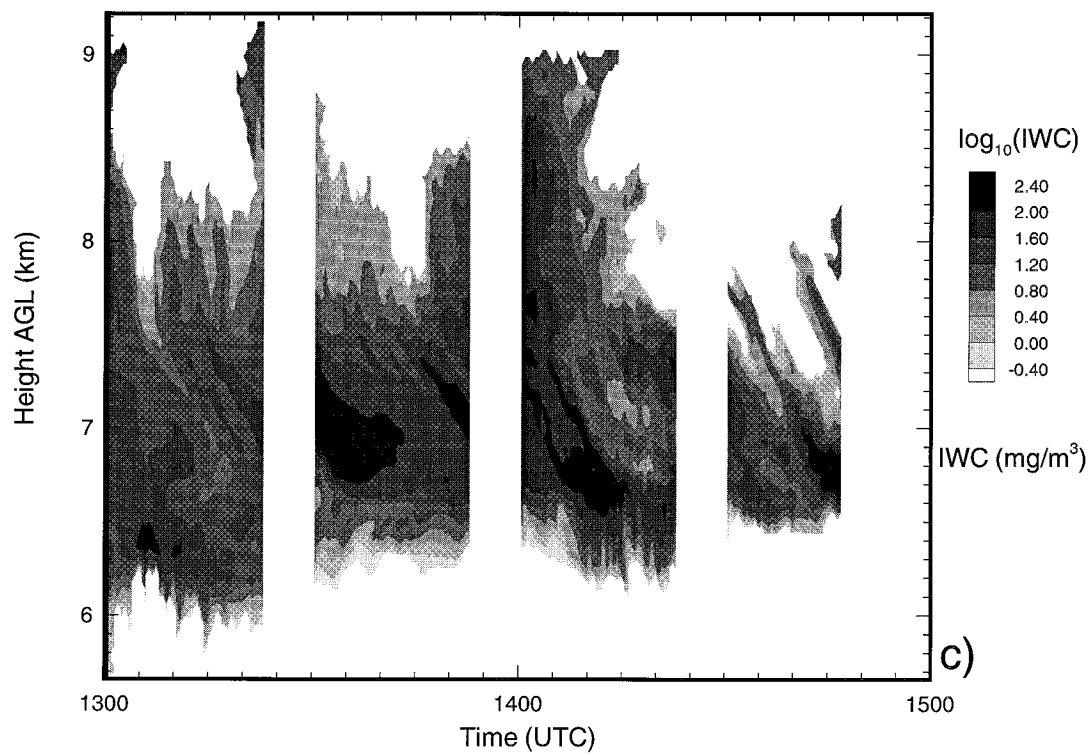


FIG. 1. (Continued)

values in this cloud reached about 7 dBZ and the weakest about -33 dBZ. The current sensitivity of the NOAA K_a -band radar allows reliable measurements of reflectivities Z_e of about -30 and -36 dBZ at 10- and 5-km altitudes, respectively. The vertical resolution of radar measurements is 37.5 m.

Figure 1b shows the retrieved field of particle median sizes D_m . The retrieved size values are quite large, which explains relatively strong reflectivities. The largest particles were usually observed in the lower part of the cloud, while the smallest particles were concentrated in the vicinity of the cloud top. This particle size stratification was repeatable in other observations, as will be shown in the next section. The smallest retrieved values of D_m are about $25 \mu\text{m}$, which is mostly dictated by the current sensitivity of the radar. Vertical fall velocities for such particles could still be up to $5\text{--}6 \text{ cm s}^{-1}$ (Mitchell 1996). Some cloud parts with smaller characteristic sizes still can be seen by the radar. However, estimates of very low reflectivity values become progressively unreliable when Z_e diminishes beyond the limits mentioned above. This may result in large retrieval errors.

The largest median sizes, D_m , observed in this ice cloud were about $400 \mu\text{m}$ near the cloud base. Existence of such large particles in the upper troposphere ice clouds is not very unusual, and it was observed during direct particle sampling in different experiments (Atlas et al. 1995; Brown et al. 1995).

Figure 1c shows the retrieved field of cloud IWC. IWC is a highly variable cloud parameter with the dynamic range of natural changes exceeding four orders of magnitude (Dowling and Radke 1990). The remotely estimated values of IWC for this cloud varied from as low as about 0.2 mg m^{-3} to as high as 0.4 g m^{-3} . The fall streaks seen in this figure were often (but not always) observed in the upper-troposphere ice clouds.

One can see that the pattern of measured radar reflectivity (Fig. 1a) and estimated IWC resemble each other. Such good correlation between Z_e and IWC, however, is not always present, as will be shown in section 5.

The number concentration of particles, N , is another cloud parameter that varies significantly. Figure 1d shows the time–height cross section of N . For the discussed cloud, particle concentrations varied from few to several hundred particles per liter. Very often the largest concentration values were retrieved for cloud parts in the vicinity of cloud tops. This can be clearly seen in Fig. 1d.

The areas of large concentrations usually reveal very small particle characteristic sizes (see Fig. 1b) and are, probably, particle-producing regions. Then particles grow as they descend through the cloud due to the diffusional growth mechanism and, perhaps, in part due to collision-coalescence processes. This results in a general increase of particle sizes and in a decrease in their number concentrations. Near the cloud base, particles begin to sublimate and larger particles usually survive longer.

A very important question concerning the microphysical retrievals is about the accuracy of estimated cloud parameters. Matrosov et al. (1994) theoretically estimated errors of retrieval results assuming reasonable uncertainties of measurements (e.g., reflectivity and brightness temperature) and different a priori assumptions (e.g., type of particle size distribution, their shape, density). This error analysis showed, in particular, that expected relative errors of particle characteristic size estimations are smaller than errors for IWC, and those for particle number concentrations are the largest from these three cloud microphysical parameters. In part, this can be explained by the large dynamic range of IWC and concentration variations compared to those for characteristic particle size. IWC and median mass particle size are relatively insensitive to small particles because the contribution of such particles in the total cloud mass is often small (Brown and Francis 1995). The total particle concentrations, on the other hand, could depend substantially on the relative amount of small particles (i.e., details of the particle size distribution).

To assess the sensitivity of retrieval results to the type of the particle size distribution, the remote sensing method was applied to the ASTEX case shown in Fig. 1 under the standard assumption of the first-order gamma distribution and also under the assumption that the distribution is exponential (Marshall–Palmer type). The exponential distribution gives a larger fraction of smaller particles compared to the first-order gamma distribution. The relative standard deviations of the D_m , IWC, and N values retrieved under these two assumptions for the whole dataset were 3%, 6%, and 60%, respectively.

In an analogous way the sensitivities to the exponent B in (4), to the assumed particle shape, and to the residual vertical air motion were estimated. A change in B from a fixed value of 0.9 to 1.1 results in the 10%, 21%, and 48% relative standard deviations in retrieved values of D_m , IWC, and N , respectively. A change in the particle aspect ratio from 0.5 to 1 (spheres) results in the 21% (D_m), 13% (IWC), and 54% (N) relative standard deviations. The residual vertical air motion of 5 cm s^{-1} would cause the standard deviation of 7%, 15%, and 35% for D_m , IWC, and N , respectively.

A more direct way to estimate accuracy of retrievals is by the comparison of remotely measured parameters with those inferred directly from balloon or aircraft. In this case both direct and remote measurements should be carefully collocated in space and time; otherwise, only qualitative conclusions can be drawn. Some comparisons of this kind were made for particle size and concentrations in Matrosov et al. (1995) and for IWC in Matrosov et al. (1996). The aircraft microphysical data were obtained using standard two-dimensional sampling techniques.

These comparisons were made for FIRE-II data and showed that retrieved and aircraft-inferred values of cloud microphysical parameters were generally in good agreement. The relative standard deviations between re-

mote and direct data were about 30% and 55% for characteristic particle sizes and IWC, respectively. Comparisons of particle concentrations from remote and direct measurements yielded the greatest discrepancy (Matrosov et al. 1995). Note that theoretical estimations and the sensitivity analysis presented above showed that retrieval uncertainties for particle concentration is much greater than those for characteristic size and IWC. More comparisons with in situ measurements should be made to better understand accuracies of the remote sensing method.

One more way to assess the performance of different remote sensing techniques is to compare simultaneous results of these techniques for retrievals of the same cloud parameter. Such comparisons are very limited at this date, however, which in part can be explained by the fact that most remote sensing methods for cloud microphysical retrievals were developed just recently. Some comparisons of characteristic cloud particle sizes obtained using the method considered here and the lidar-radar backscatter ratio technique were given by Matrosov et al. (1995).

4. Vertical variability of cloud microphysics

Both the shortwave and the longwave components of the radiation budget are sensitive to the vertical distribution of cloud parameters. In this section, the vertical variability of particle characteristic sizes and IWC is discussed. These parameters are the most important microphysical properties for modeling cloud radiative effects.

The variability is illustrated by results obtained during the observational cases in FIRE-II, ASTEX, and the Arizona Program. Only three cases were chosen here for each experiment from many processed datasets. These were selected as the most representative cases in terms of event duration, cloud geometrical thickness, and radar reflectivity magnitudes. The volume of data points for each case varied from about 2000 for the 18 June 1992 ASTEX case to about 20 000 for the 26 November 1991 FIRE-II case.

a. Variability of median particle size

Figure 2 shows scatterplots of retrieved values of cloud particle median sizes, D_m , as a function of height. As before, D_m refers to a spherical particle of equal volume. As for data in Fig. 1, it was assumed during retrievals that cloud particles are a mixture of 50% prolate (columnar-type crystals) with 50% oblate (planar-type crystals). The general decrease of the cloud particle bulk density with the increase of their size was accounted for by the use of (5). The size distribution of particles was assumed to be the gamma function of the first order. The sensitivity of the retrieval results to these assumptions was discussed in the previous section.

The dates and times of observations are shown inside

each panel in Fig. 2. The 1991, 1992, and 1995 cases belong to FIRE-II, ASTEX, and the Arizona Program, respectively. The duration of different cases varied from 1.2 to 3 h. For easier comparisons, the vertical and horizontal scales are the same in all the panels. The observed clouds were located between 5.6 and 11.4 km above the ground. No significant amount of liquid water was detected in any of these clouds (as reported by microwave radiometers); however, some traces of liquid could be present in lower parts of the cloud observed on 3 March 1995. Only liquid-free cloud volumes above 5.6 km were used for the retrievals in that case.

Each scatterplot in Fig. 2 represents superimposed, individual, vertical profiles of D_m retrieved during the whole observational period with the time resolution of 30 s. The middle solid curve in each panel shows the mean profile $\langle D_m \rangle$, and the left and right curves depict profiles representing $\langle D_m \rangle \pm SD$, where SD is the standard deviation. The temperature reference points known from radiosonde soundings are shown on the altitude axes. The vertical temperature gradient inside clouds was assumed to be constant.

The vertical limits of the data area coincide with the highest and lowest radar range gates where cloud was detected during the observational event. Geometrical thickness of clouds at individual time moments varied from about a few hundred meters to about 3.5 km. Similar thickness changes for ice clouds in the upper troposphere were reported by Machover and Nudelman (1989). Most of the clouds were one-layer clouds with cloud boundaries changing over time. The cloud of 14 November 1991, however, consisted of two layers that could be seen in Fig. 2a.

It can be seen from Fig. 2 that the general behavior of mean vertical profiles of particle characteristic sizes is very similar in all the observed clouds. Generally D_m is increasing monotonically toward the cloud base. However, in a lower few radar range gates, particle sizes decrease approaching to the cloud base, which indicates sublimation. Values of standard deviations from the mean profiles are generally a factor of 2 or 3 smaller than the mean values. The vertical variability of D_m from small particles near the cloud top to larger particles near the cloud base, even in mean profiles, can reach one order of magnitude. The vertical variability in individual profiles can be even greater when the difference between D_m at the cloud top and base can exceed one order of magnitude.

b. Variability of cloud ice mass content

Figure 3 illustrates the vertical variability of retrieved profiles of IWC. Data are shown for the same experimental cases from FIRE-II, ASTEX, and the Arizona Program as in Fig. 2. One can see that the variability in IWC is usually much greater than that of particle characteristic sizes and can reach several orders of magnitude (up to two orders of magnitude for mean profiles

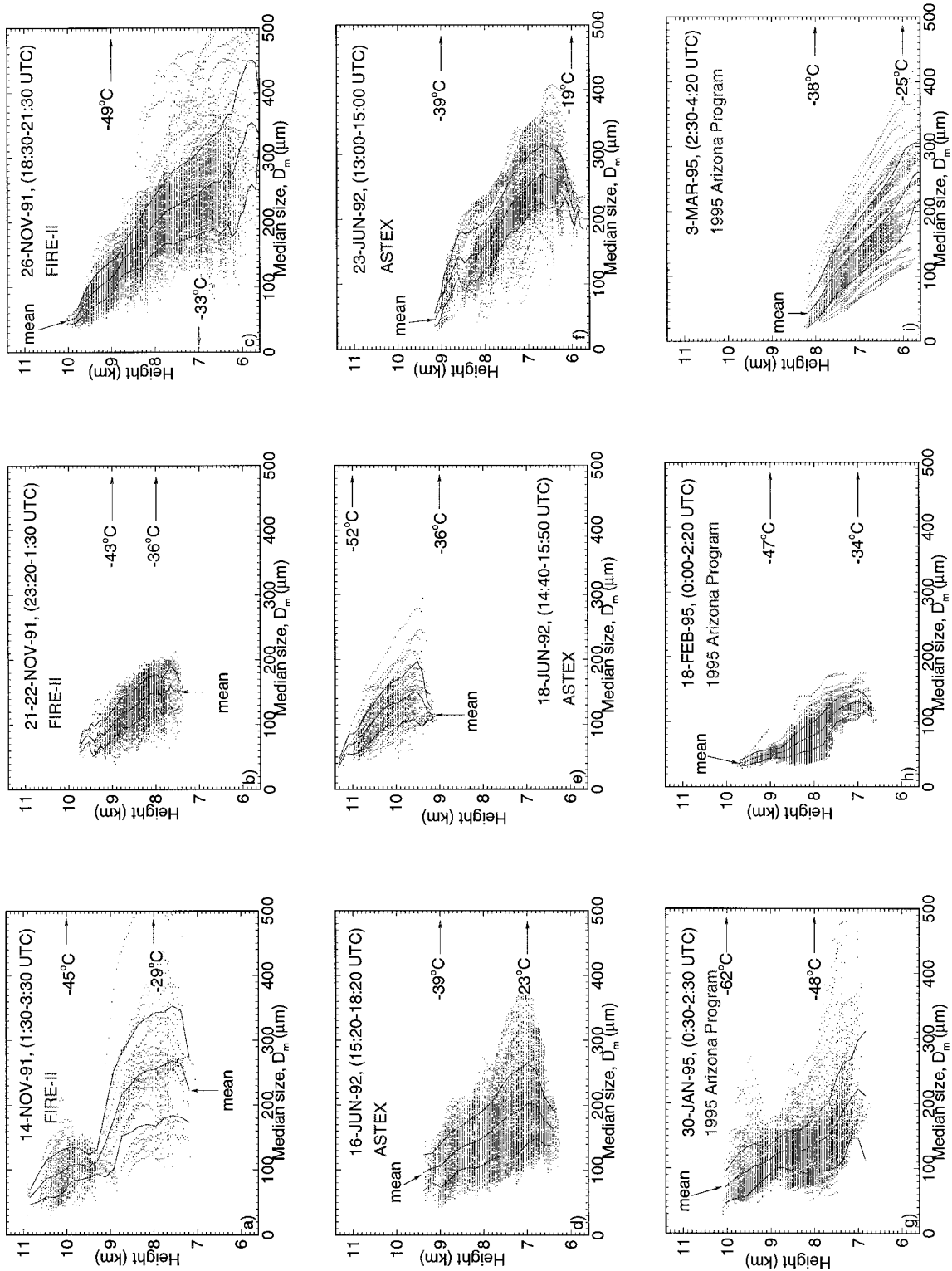


FIG. 2. Scatterplots of particle median sizes for different observational cases from FIRE-II (a), (b), (c); ASTEX (d), (e), (f); and the 1995 Arizona Program (g), (h), (i). Middle curves show mean profiles (D_m), and right and left curves show profiles for $\langle D_m \rangle + \text{SD}$ and $\langle D_m \rangle - \text{SD}$, where SD is the standard deviation.

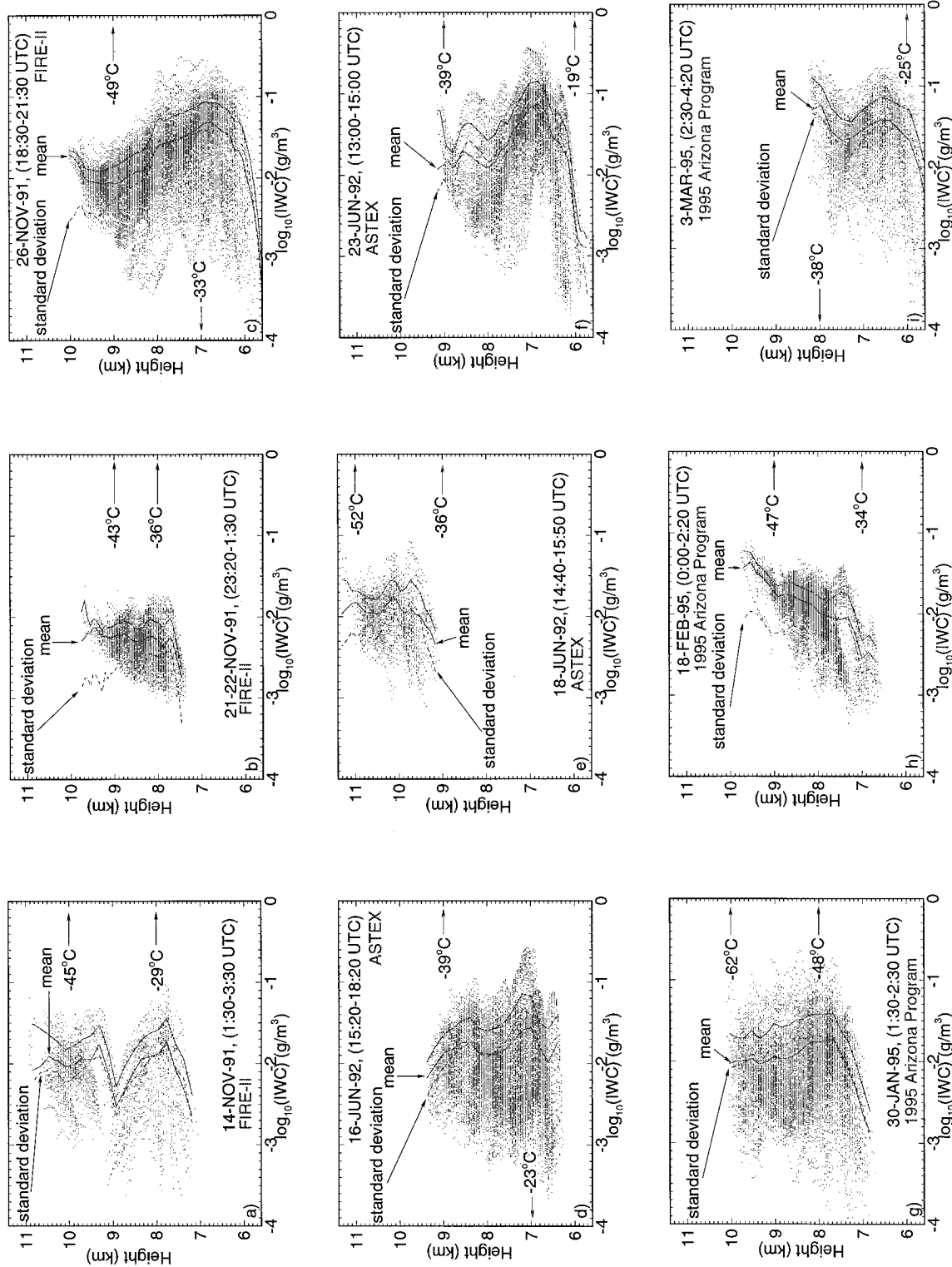


FIG. 3. Scatterplots of IWC for different observational cases from FIRE-II (a), (b), (c); ASTEX (d), (e), (f); and the 1995 Arizona Program (g), (h), (i). Left solid curves show mean profiles (IWC), right solid curves show profiles for (IWC) + SD, and dashed curves show profiles of standard deviation (SD).

and up to four orders of magnitude in individual profiles). The bulk of IWC data is in the range from 0.1 to 0.001 g m⁻³. Some cloud parts with very low IWC are probably missed due to the current sensitivity of the NOAA K_a-band radar.

Mean vertical profiles ⟨IWC⟩ shown by the left solid curves do not follow a consistent pattern. Some profiles, like those for D_m , exhibit an increase of IWC in the lower part of the cloud (e.g., 23 June 1992, 30 January 1995), while the others show almost neutral vertical distribution (e.g., 21–22 November 1991, 18 June 1992) or an increase in the upper part of the cloud (e.g., 18 February 1995). One common feature for all the profiles is a rapid decrease of IWC in the nearest vicinity of the cloud base, reflecting quick sublimation.

An important difference between vertical variability of IWC and vertical variability of D_m is the magnitude of standard deviations from mean profiles. For IWC, values of standard deviations are close to mean values and sometimes exceed them (e.g., 30 January 1995). Because of this fact, the profiles of ⟨IWC⟩ – SD are not shown. The solid right curves depict profiles of ⟨IWC⟩ + SD and dashed curves show the profiles of SD. Large relative values of SD for IWC reflect the much greater natural variability of IWC compared with the natural variability of cloud particle characteristic size.

As was mentioned before, possible retrieval errors for IWC are generally greater than those for D_m (Matrosov et al. 1994) and they increase for smaller particle sizes. Therefore, the uncertainty in the IWC values in the upper few range gates is usually greater than that in the middle or lower part of a cloud.

5. Variability of relations between reflectivity and cloud microphysical parameters

Recent advances in millimeter-wavelength radar applications for studying nonprecipitating ice clouds induced a wide interest in developing empirical relationships between cloud microphysical parameters and radar reflectivity based on the regression analysis. However, retrievals based on multisensor observations are more robust than those based on these relationships that usually are sought in the form of power-law regressions:

$$\text{IWC} = a_1 Z_e^b, \quad (6)$$

$$D_m = a_2 Z_e^c, \quad (7)$$

where a_1 , a_2 , b , and c are the regression coefficients.

In situations when the multisensor approach is not available for some reason and radar reflectivity data only are used, such regressions could be helpful. One, however, should realize the limitation of the regression approach due to the variability of the relationships between microphysical parameters and reflectivity from cloud to cloud (Atlas et al. 1995).

The most attention recently has been given to de-

veloping empirical power-law regressions between IWC and radar reflectivity Z_e . Usually such regressions are deduced from measured particle spectra when both IWC and Z_e are calculated from these spectra. Particle samples are usually taken from research aircraft or on the ground. Some recent publications on this subject include Brown et al. (1995), Liao and Sassen (1994), Sassen and Liao (1996).

Figure 4 shows IWC– Z_e power-law regressions from these recent studies and also one obtained from aircraft sampling during the FIRE-I experiment (Atlas et al. 1995). It should be noted that the spread in individual regressions is about one order of magnitude for a typical reflectivity –20 dBZ. The results for W ($\lambda \approx 3$ mm) and K_a bands obtained from the same dataset are rather close (curves 3 and 5), which shows that non-Rayleigh scattering effects are very small for nonprecipitating ice clouds at these frequencies. A similar conclusion was also obtained theoretically (Matrosov 1993).

Usually, an empirical IWC– Z_e power-law regression for a particular dataset is derived for a wide region of reflectivity and IWC. However, in practice the relation between IWC and Z_e can vary depending on the magnitude of these parameters even for the same observational case. In order to illustrate this point, Fig. 4 shows also IWC– Z_e stratified approximations for two ice cloud cases considered here (23 June 1992 ASTEX and 3 March 1995 Arizona Program). These approximations were obtained independently for short intervals of IWC and are discussed in more detail in the next subsection.

It has been shown, for ice clouds (Atlas et al. 1995), that reflectivity can be expressed in terms of IWC and D_m as

$$Z_e = G \text{IWC} D_m^3, \quad (8)$$

where G is a dimensionless parameter that depends on the particle size distribution type, density, and shape. The major influence on Z_e is, however, exercised by IWC and D_m . The reflectivity dependence on the other factors is generally smaller and, with some uncertainty, can be accounted for by reasonable assumptions. The main reason for the spread in empirical power-law regressions shown in Fig. 4 is, most likely, due to different particle characteristic sizes for individual datasets that were used to derive these different IWC– Z_e regressions. Likewise, the spread in D_m – Z_e regressions would be caused mainly by variations in IWC.

One can expect some positive correlation between IWC and D_m that would reduce the spread in the empirical relationships compared with the case if IWC and D_m were completely uncorrelated. The multisensor approach uses other measurables (e.g., IR, Doppler information) to get independent estimates of IWC and D_m .

a. Variability of IWC– Z_e relationships

In order to compare with existing empirical regressions, the best fit power-law IWC– Z_e regressions were

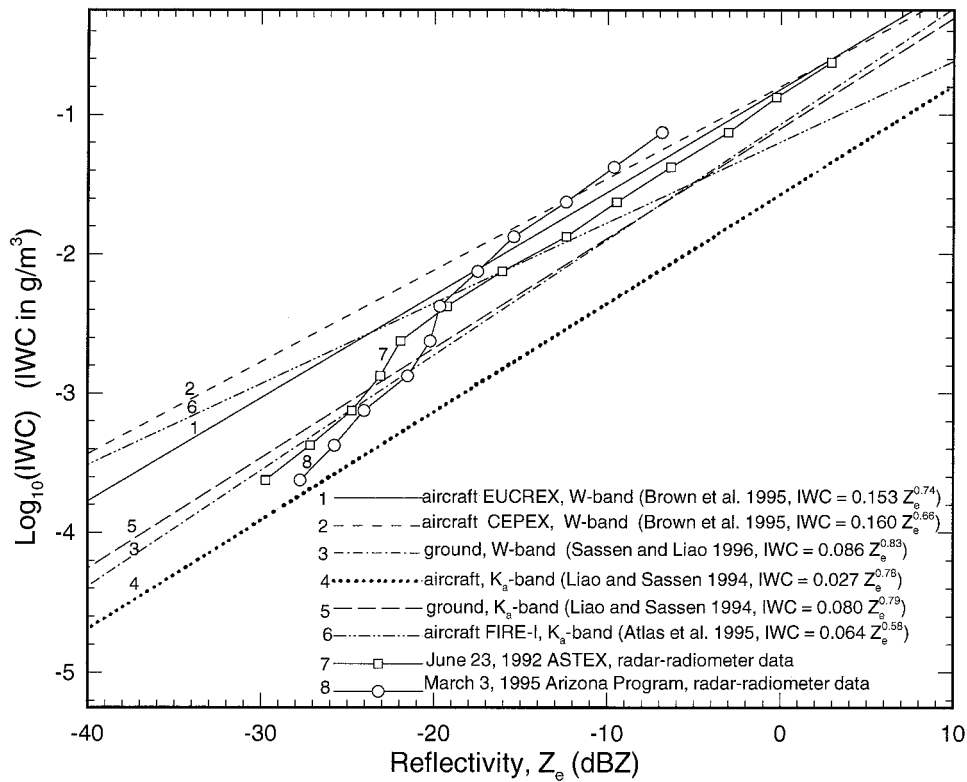


FIG. 4. Different empirical power-law IWC- Z_e relationships [Eqs. (1)–(6)] and stratified approximations for 23 June 1992 and 3 March 1995 obtained using the radar-radiometer method.

derived for all the experimental cases discussed in the previous section. Measured values of reflectivity Z_e and values of IWC derived from combined radar and radiometer measurements were used to construct such regressions. For a valid comparison, power-law regressions for the cases considered here were also constructed for whole dynamic range of observed Z_e and retrieved IWC assuming the same statistical weight for all the data points. Table 1 presents values of the coefficients a_1 and b for the power-law regression (6) for this case. Also presented in Table 1 are the relative standard deviations S_d of regression results from IWC estimated using the multisensor approach

$$S_d^2 = \frac{1}{M} \sum_i \frac{(a_1 Z_{ei}^b - IWC_i)^2}{IWC_i^2}, \quad (9)$$

where M is the number of data points. The units of the coefficients a_1 and b assume that IWC is in grams per cubic meter and Z_e is in its standard units ($\text{mm}^6 \text{m}^{-3}$).

Values of a_1 from Table 1 vary from 0.042 to 0.219, which is in general accord with data from Fig. 4. The coefficient b varies from 0.29 to 0.70 if all the reflectivities are considered. However, if only reflectivities with $Z_e > -20$ dBZ are taken into account, the variability of b diminishes to 0.43–0.74. Note that uncertainty of IWC retrievals is greater for weaker reflectiv-

TABLE 1. Coefficients in the power law regression $IWC = a_1 Z_e^b$ and its standard deviations S_d .

Date	For all reflectivities			For reflectivities $Z_e \geq -20$ dBZ		
	α_1	b	S_d	α_1	b	S_d
14 November 1991	0.042	0.42	154%	0.041	0.43	111%
21–22 November 1991	0.052	0.48	38%	0.090	0.61	23%
26 November 1991	0.084	0.56	84%	0.093	0.60	57%
16 June 1992	0.127	0.67	68%	0.117	0.64	60%
18 June 1992	0.092	0.50	69%	0.106	0.53	43%
23 June 1992	0.112	0.68	63%	0.120	0.73	42%
30 January 1995	0.219	0.70	192%	0.246	0.74	130%
18 February 1995	0.045	0.29	146%	0.238	0.67	34%
3 March 1995	0.095	0.48	186%	0.100	0.50	90%

ities. There is a weak general tendency for b to increase when stronger reflectivities are considered.

The relative standard deviation (9) expressed in percent varied from almost 200% to about 40%, showing that the quality of the power-law regression varies from cloud to cloud. Figure 5 illustrates this point. Two observational cases are presented in this figure. The ASTEX 23 June 1991 case shown as an example of the retrievals in section 3 is characterized by a high correlation between reflectivity and IWC. This correlation is also evident in the similarity of the Z_e and IWC fields presented in Fig. 1a and 1c, respectively. The corresponding correlation coefficient is about 0.9 for this case. Despite the good correlation and relatively low S_d , deviations of individual data points from the regression line could be significant, especially for low reflectivities.

In addition to the power-law regression for all the data points for this case, a stratified approximation was constructed for data points in 12 IWC intervals separated by 0.25 in logarithmic scale starting from $\log_{10}(\text{IWC}) = -0.5$ (IWC is in grams per cubic meter). Mean values of reflectivity ($\text{mm}^6 \text{m}^{-3}$) were calculated for each of the IWC intervals. These values are shown in Fig. 5 as symbols. One can see that for the ASTEX case (Fig. 5a), the stratified approximation follows the general power-law regression quite well except for very small IWC and Z_e . The tendency of increasing b as stronger reflectivities are considered can also be seen in these figures.

Contrary to that, the Arizona Program 3 March 1995 experimental case (Fig. 5b) does not exhibit a high correlation between Z_e and IWC, with the correlation coefficient being about 0.65. One can also see from Fig. 5b that the slope of the power-law regression (b) will increase and standard deviation will decrease if data points with higher reflectivities are considered. Comparisons of the stratified approximation with the power-law regression for all the data points show that the relation between IWC and reflectivity for this case varied significantly depending on the absolute values of parameters. As in the previous case, the largest differences in the relation for this case are for smaller values of Z_e .

Data from Table 1 and Fig. 4 indicate that values of b (especially for $Z_e > -20$ dBZ) are mostly from 0.53 to 0.74. However, values of a_1 vary more significantly. Based on this fact, an idea of "tuning" power-law IWC- Z_e regressions can be suggested. If the coefficient b is set for some reasonable value (around 0.65–0.70), the value of a_1 can be tuned for a particular profile if an independent measure of the vertical integral of IWC-ice water path (IWP) is available. In this situation no vertical Doppler measurements are needed, and profiles of IWC can be estimated from reflectivity measurements. This will eliminate problems arising from the need of averaging Doppler information and constructing regressions between particle fall velocities, reflectivities, and heights using the approach by Orr and Kropfli

(1993). A potential payoff for such simplification could be a possible sacrifice in the retrieval accuracy.

IWP for each profile can be estimated without the use of Doppler information. It could be done from the mean reflectivity and IR brightness (Matrosov et al. 1992) for ground-based measurements or from multichannel submillimeter radiometer measurements for satellite measurements (Evans and Stephens 1995). Some further studies are needed to investigate the possibilities of "tuning" IWC- Z_e and possible trade-offs.

b. Variability of D_m - Z_e relationships

Power-law D_m - Z_e regressions were derived in the same way as power-law IWC- Z_e regressions for the experimental cases discussed above. Values of coefficients a_2 and c in (7), as well as standard deviations S_d calculated using an equation analogous to (9), are presented in Table 2. The units of a_2 and c are such that D_m in (7) is in microns and Z_e is in the aforementioned units ($\text{mm}^6 \text{m}^{-3}$). Case-to-case variations of the coefficient a_2 are less than those for a_1 in (6). The standard deviations here are also considerably less than for the IWC- Z_e relationships, which can be explained, in part, by the smaller natural variations of particle characteristic sizes compared to those of IWC. An average value of the coefficient c is about 0.2.

Figure 6 shows scatterplots of retrieved particle sizes versus measured reflectivities for the same experimental cases as in Fig. 5. Here again, the ASTEX 23 June case exhibits greater correlation than the Arizona-95 3 March case. The correlation coefficients for these cases are 0.75 and 0.65, respectively. The values of a_2 happened to be close for these cases. However, as can be seen from Table 2, the variability of this coefficient is still significant.

As for IWC- Z_e relationships, stratified approximations of the D_m - Z_e relationships were also constructed here. It was done for $\log_{10}(D_m)$ intervals of 0.1 (D_m in microns). These approximations are also shown in Fig. 6. Comparisons of stratified approximations and power-law regressions for all the data points show much greater variability of the relation between reflectivity and cloud particle size for the Arizona case compared to the ASTEX case. As for IWC, the greatest differences are seen for lower reflectivities. When comparing Figs. 5 and 6 one should have in mind a much greater dynamic range of the y axis in Fig. 5 compared to Fig. 6.

Similar to the procedure proposed in the previous subsection, "tuning" the power-law D_m - Z_e regressions can be also suggested. As a normalizing factor for each vertical profile, vertically averaged particle characteristic sizes can be used. The vertically averaged values of D_m are available from averaged reflectivity and IR brightness (Matrosov et al. 1992). Such approach will avoid the use of Doppler information and problems of time averaging of vertical velocities.

A possible increase in uncertainty of remotely mea-

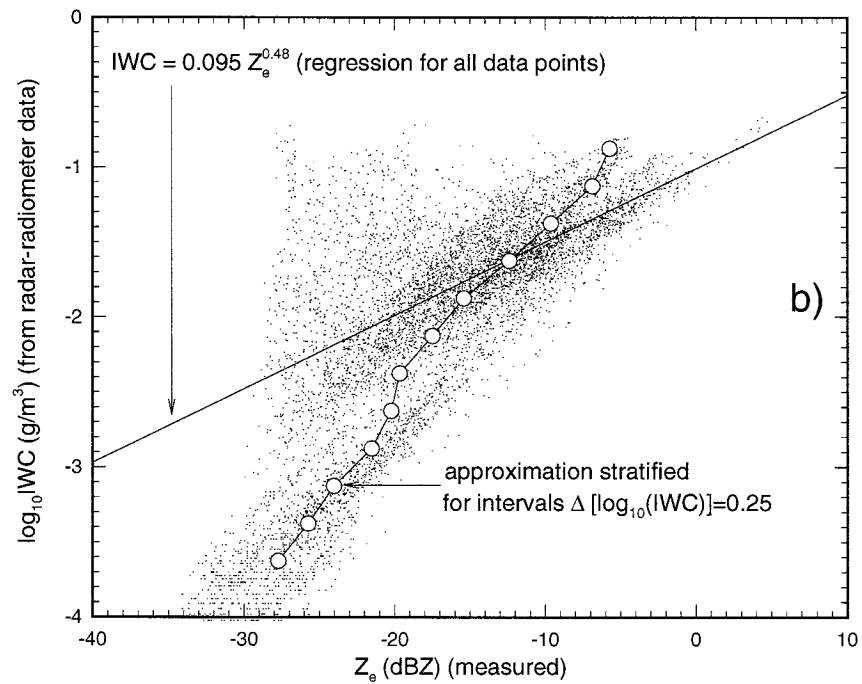
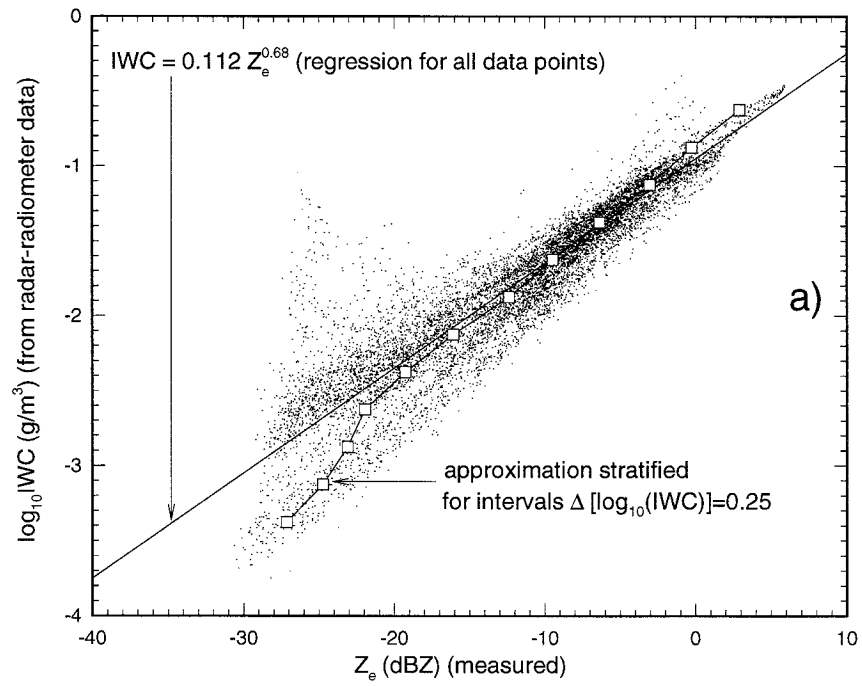


FIG. 5. Scatterplot of IWC retrieved from radar-radiometer measurements versus measured radar reflectivity Z_e , (a) 23 June 1992, (b) 3 March 1995.

TABLE 2. Coefficients in the power-law regression $D_m = a_2 Z_e^c$ and its standard deviations S_d .

Date	For all reflectivities			For reflectivities $Z_e > -20$ dBZ		
	a_2	c	S_d	a_2	c	S_d
14 November 1991	480	0.27	39%	499	0.28	34%
21–22 November 1991	455	0.25	19%	329	0.18	14%
26 November 1991	345	0.22	26%	337	0.19	20%
16 June 1992	290	0.16	28%	301	0.17	23%
18 June 1992	331	0.23	26%	319	0.22	18%
23 June 1992	307	0.15	27%	297	0.13	18%
30 January 1995	223	0.14	35%	216	0.13	29%
18 February 1995	345	0.28	28%	244	0.19	16%
3 March 1995	322	0.23	40%	325	0.23	31%

sured vertical profiles of cloud properties due to the suggested simplifications should be carefully estimated and understood. This can be done by comparing results obtained using the full method and its simplified version. Such comparisons should be based on analyses of clouds at different conditions and on more extensive verifications of remote and direct in situ measurements that are available now.

6. Conclusions

The remote sensing method to retrieve ice cloud microphysical parameters from combined measurements taken by the vertically pointed Doppler K_a -band radar and the narrowband IR-radiometer was applied for different experimental situations from FIRE-II, ASTEX, and the Arizona Program experiments. The observed clouds were predominantly ice-phase clouds in the upper troposphere between about 5.6 and 11 km with a typical thickness of about 2 km. Each cloud was observed during time period from about 1.2 to 3 h as it advected above the ground-based instruments.

Mean vertical profiles of the cloud median mass size D_m and ice mass content were constructed for each discussed case. Values of retrieved sizes D_m varied from about 25 to 400 μm . A typical vertical profile of D_m exhibits a gradual increase of particle characteristic size toward the cloud base. In the vicinity of the cloud top, particles are usually the smallest and their concentration is the highest. The last few range gates at the cloud base show a sharp decrease in particle sizes and concentrations due to fast sublimation. Changes of D_m for a mean vertical profile can reach and for an individual profile even exceed one order of magnitude. Standard deviations from mean size profiles usually are smaller than mean values by a factor of 2 or 3 depending on the altitude.

Mean vertical profiles of IWC do not exhibit an obvious preference to reach a maximum value in a particular cloud part. Sometimes, but not always, IWC changes relatively slightly along the fall streaks. A rapid decrease of IWC due to sublimation is evident in the vicinity of cloud bases. IWC shows a much greater variability than the particle characteristic size. Standard de-

viations of IWC profiles are close and in many instances exceed mean values at corresponding levels. The variability of retrieved values of IWC for the analyzed observational cases reached about four orders of magnitude; however, the bulk of the IWC data were from 1 to 100 mg m^{-3} .

The power-law regressions between measured radar reflectivities Z_e and cloud microphysical parameters were estimated. Parameters of these regressions are in a general agreement with those obtained by direct analysis of particle spectra. These parameters show a significant variability from one experimental case to another. These parameters could change if different intervals of reflectivity and estimated microphysical properties are considered.

The variability of the exponent coefficients (b and c) is generally less than one of the coefficients a_1 and a_2 (especially for IWC– Z_e power-law regressions). Based on this fact, a procedure of “tuning” these regressions was suggested. Such “tuning” requires knowing IWP and the vertically averaged particle characteristic size, which can be estimated without the use of Doppler velocity measurements. This can eventually lead to a simplification of the radar–radiometer remote sensing method. However, a potential increase in uncertainties of retrieved cloud microphysical parameters should be carefully estimated.

The observational cases presented in this paper are somewhat typical, in terms of event durations, cloud boundaries heights, and observed reflectivity values, for a larger number of cloud situations analyzed using the radar–radiometer remote sensing method. For climatological purposes, however, much more extensive information is required. In this view, the remote sensing method should be applied to long-term continuous datasets. Such datasets could be available, for example, through the Atmospheric Radiation Measurement (ARM) Program where active and passive instruments similar to those of ETL are deployed at several geographical locations for long-term period atmospheric observations.

The application of the current version of the radar–radiometer remote sensing method requires, however, certain conditions (e.g., the absence of low-level clouds,

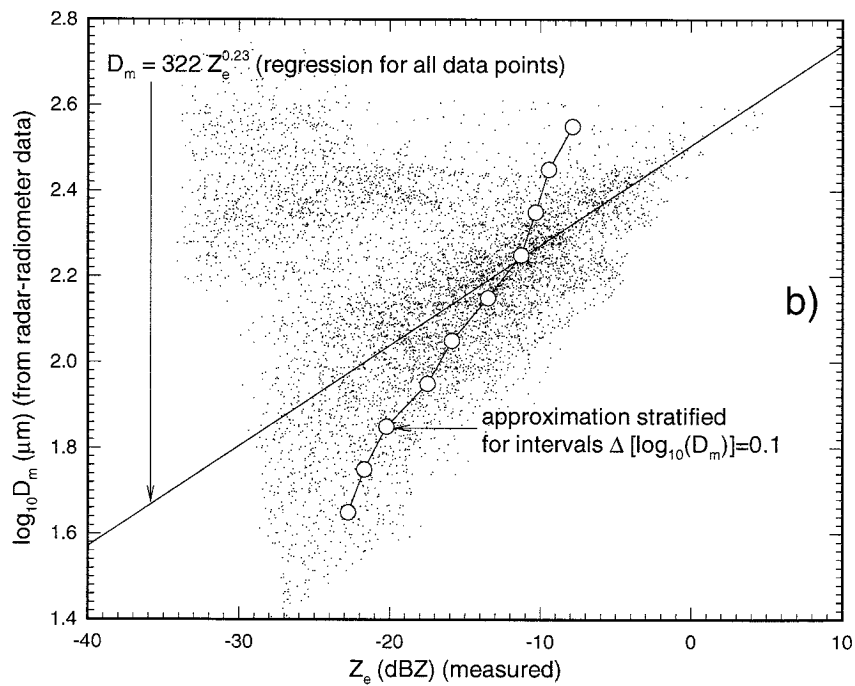
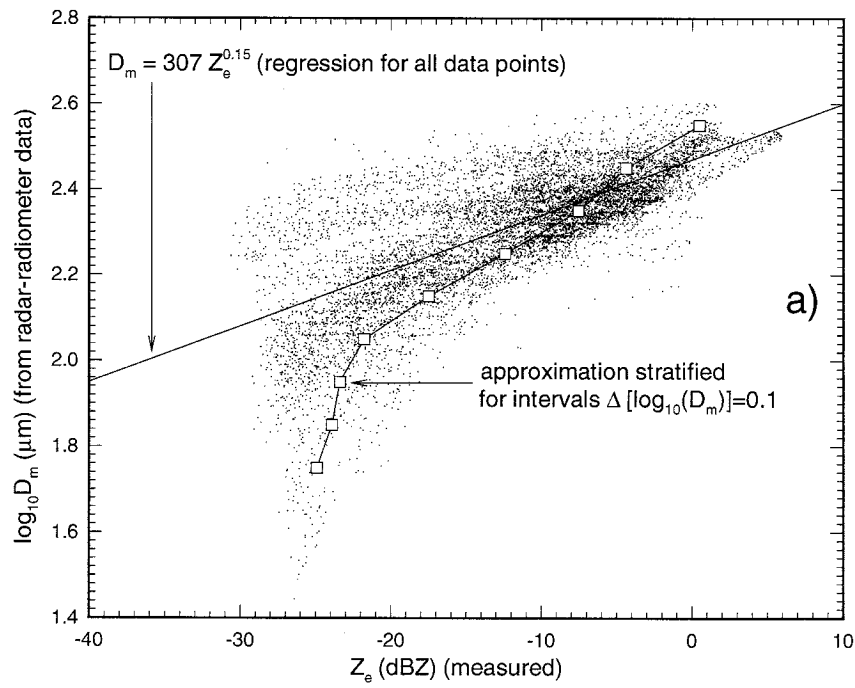


FIG. 6. Same as in Fig. 5 but for particle median size D_m .

persistence of the cloud) and preliminary screening of suitable situations (e.g., in terms of absence of strong turbulence, which would hamper estimating the particle terminal fall velocities). This requires further technique development in order to automate the remote sensing method and, probably, to develop some simplified versions that could be applicable in more situations (e.g., “tuning” of the power-law relationships between cloud microphysical parameters and radar reflectivity). The accuracy trade-offs of such simplifications, however, should be assessed.

Acknowledgments. This work was supported by the Environmental Science Division of the U.S. Department of Energy as part of the Atmospheric Radiation Measurement Program. The author would like to thank R. A. Kropfli, T. Uttal, B. E. Martner, R. F. Reinking, B. W. Orr, and I. Gulpepe for valuable discussions through the course of the work. B. W. Bartram and K. A. Clark were operating the ETL K_a -band radar, and J. B. Snider provided the radiometric data.

REFERENCES

- Atlas, D., S. Y. Matrosov, A. J. Heymsfield, M. D. Chou, and D. B. Wolff, 1995: Radar and radiation properties of ice clouds. *J. Appl. Meteor.*, **34**, 2329–2345.
- Brown, P. R. A., and P. N. Francis, 1995: Improved measurements of the ice water content in cirrus using a total-water probe. *J. Atmos. Oceanic Technol.*, **12**, 410–414.
- , A. J. Illingworth, A. J. Heymsfield, G. M. McFarquhar, K. A. Browning, and M. Gosset, 1995: The role of spaceborne millimeter-wave radar in the global monitoring of ice cloud. *J. Appl. Meteor.*, **34**, 2346–2366.
- Chylek, P., and G. Videen, 1994: Longwave radiative properties of polydispersed hexagonal ice crystals. *J. Atmos. Sci.*, **51**, 175–190.
- Clothiaux, E. E., M. A. Miller, B. A. Albrecht, T. P. Ackerman, J. Verlinde, D. M. Babb, R. M. Peters, and W. Syrett, 1995: An evaluation of a 94-GHz radar for remote sensing of cloud properties. *J. Atmos. Oceanic Technol.*, **12**, 210–229.
- Dowling, D. R., and L. F. Radke, 1990: A summary of the physical properties of cirrus clouds. *J. Appl. Meteor.*, **29**, 970–987.
- Evans, K. F., and G. L. Stephens, 1995: Microwave radiative transfer through clouds composed of realistically shaped ice crystals. Part II: Remote sensing of ice clouds. *J. Atmos. Sci.*, **52**, 2058–2072.
- Hobbs, P. V., Ed., 1993: *Aerosol-Cloud-Climate Interactions*. Academic Press, 234 pp.
- IGPO, 1994: Utility and feasibility of a cloud profiling radar. IGPO Publication Series, 1994. Rep. of the GEWEX Topical Workshop N 10, WMO/TD-No. 593, WCRP-84, 92 pp. [Available from World Meteor. Org., Publications Sales Unit, Case Postale 2300, CH-1211 Geneva 2, Switzerland.]
- Intrieri, J. M., W. L. Eberhard, T. Uttal, J. A. Shaw, J. B. Snider, Y. Han, B. W. Orr, and S. Y. Matrosov, 1995: Multiwavelength observations of a developing cloud system: The FIRE-II 26 November case study. *J. Atmos. Sci.*, **52**, 4079–4093.
- Klimowski, B. A., 1995: The 1995 Arizona program. Field operation plan, 67 pp. [Available from Department of Atmospheric Sciences, University of Arizona, Tucson.]
- Kosarev, A. L., and I. P. Mazin, 1989: Empirical model of physical structure of the upper level clouds of the middle latitude. *Radiation Properties of Cirrus Clouds* (in Russian). E. Feigelson, Ed., Nauka, 29–52.
- Kropfli, R. A., and R. D. Kelly, 1996: Meteorological research applications of mm-wave radar. *Meteor. Atmos. Phys.*, **59**, 105–121.
- , S. Y. Matrosov, T. Uttal, B. W. Orr, A. S. Frisch, K. A. Clark, B. W. Bartram, R. F. Reinking, J. B. Snider, and B. E. Martner, 1995: Cloud physics studies with 8-mm wavelength radar. *Atmos. Res.*, **35**, 299–313.
- Liao, L., and K. Sassen, 1994: Investigation of relationships between Ka-band radar reflectivity and ice and liquid water content. *Atmos. Res.*, **34**, 231–248.
- Machover, Z. M., and L. A. Nudelman, 1989: Climatology of upper layer clouds. Review of their microphysical and optical properties. *Radiation Properties of Cirrus Clouds* (in Russian). E. Feigelson, Ed., Nauka, 6–31.
- Matrosov, S. Y., 1993: Possibilities of cirrus particle sizing from dual-frequency radar measurements. *J. Geophys. Res.*, **98**, 20 675–20 683.
- , and J. B. Snider, 1995: Studies of cloud ice water content and optical thickness during FIRE-II and ASTER. *Proc. SPIE*, **2578**, 133–137.
- , T. Uttal, J. B. Snider, and R. A. Kropfli, 1992: Estimation of ice cloud parameters from ground-based infrared radiometer and radar measurements. *J. Geophys. Res.*, **97**, 20 675–20 683.
- , B. W. Orr, R. A. Kropfli, and J. B. Snider, 1994: Retrieval of vertical profiles of cirrus cloud microphysical parameters from Doppler radar and infrared radiometer measurements. *J. Appl. Meteor.*, **33**, 617–626.
- , —, J. M. Intrieri, B. W. Orr, and J. B. Snider, 1995: Ground-based remote sensing of cloud particle sizes during the 26 November 1991 FIRE II cirrus case: Comparisons with in situ data. *J. Atmos. Sci.*, **52**, 4128–4142.
- , A. J. Heymsfield, R. A. Kropfli, and J. B. Snider, 1996: Comparisons of cloud ice mass content retrieved from radar-IR radiometer method with aircraft data during the Second International Satellite Cloud Climatology Project Regional Experiment (FIRE-II). *Proc. 5th Atmospheric Radiation Measurement Science Team Meeting*, San Diego, CA, U.S. Department of Energy, 189–192.
- Mead, J. B., A. L. Pazmany, S. M. Sekelsky, and R. E. McIntosh, 1994: Millimeter-wavelength radars for remotely sensing clouds and precipitation. *Proc. IEEE*, **82**, 1891–1906.
- Mitchell, D. L., 1996: Use of mass- and area-dimensional power laws for determining precipitation particle terminal velocities. *J. Atmos. Sci.*, **53**, 1710–1723.
- Orr, B. W., and R. A. Kropfli, 1993: Estimation of cirrus cloud particle fall speeds from vertically pointing Doppler radar. Preprints, *26th Int. Conf. on Radar Meteorology*, Norman, OK, Amer. Meteor. Soc., 588–590.
- Platt, C. M. R., and A. C. Dilley, 1979: Remote sounding of high clouds: II. Emissivity of cirrostratus. *J. Appl. Meteor.*, **18**, 1144–1150.
- Randall, D. A., 1995: Atlantic Stratocumulus Transition Experiment. *J. Atmos. Sci.*, **52**, 2705–2706.
- Sassen, K., and L. Liao, 1996: Estimation of cloud content by W-band radar. *J. Appl. Meteor.*, **35**, 932–938.
- Stephens, G. L., 1995: First ISCCP regional experiment: Intensive field operations II. *J. Atmos. Sci.*, **52**, 4041–4042.